SMA CONTROL FOR BIO-MIMETIC FISH LOCOMOTION

Claudio Rossi, Antonio Barrientos
Robotics and Cybernetics Research Group, Universidad Politécnica de Madrid, Madrid, Spain
claudio.rossi@upm.es, antonio.barrientos@upm.es

William Coral Cuellar
Dep. Génie Électrique et Sistèmes de Commande , Université de Technologie de Belfort-Montbéliard , Belfort, France
William.Coral@utbm.fr

Keywords: Shape Memory Alloys, Biologically-Inspired Robots, Smart Actuators control, Underwater Robotics.

Abstract: In this paper, we describe our current work on bio-inspired locomotion systems using smart materials. The aim of this work is to investigate alternative actuation mechanisms based on smart materials, exploring the possibility of building motor-less and gear-less robots. A swimming underwater robot is being developed whose movements are generated using such materials, concretely Shape Memory Alloys. This paper focuses on the actuators control in order to generate the desired motion patterns.

1 INTRODUCTION

Robotics actuator technology is basically dominated by two kind of actuators: electric motors/servomotors and pneumatic/hydraulic actuators. In mobile robotics, the former is mostly used, with exceptions being e.g. large legged robots (de Santos et al., 2007). The (rotatory) motion of the motors is then transmitted to the effectors through gearboxes, belts and, in the case linear actuation is needed, other mechanic devices. Although applied with success in uncountable robotic devices, such systems can be complex, heavy and bulky[1]. In underwater robots, propellers are most used for locomotion an maneuvering. Propellers however may have problems of cavitation, noise, efficiency and danger for sea life.

Underwater creatures are capable of high performance movements in water. Thus, underwater robot design based on the movement mechanism of fishes appears to be a promising approach. Over the past few years, researches have been developing underwater robots based on underwater creatures swimming mechanism (Hu, 2006), (Anderson and Chhabra, 2002), (Morgansen et al., 2007). Yet, most of them still rely on servomotor technology and a structure made of a discrete number of elements. One of the most advanced robot fishes is the MIT fish (Valdivia y Alvarado and Youcef-Toumi, 2006). This fish has a continuous soft body. A single motor generates a wave that is propagated backward in order to generate propulsion.

Recently, new actuation technology in active or ”smart” materials has opened new horizons as far as simplicity, weight and dimensions. New materials such as piezo-electric fiber composite, electro-active polymers and shape memory alloys (SMA) are being investigated as a promising alternative to standard servomotor technology. The potential gain in weight and dimension would allow building lighter and smaller robots, and even devising soft-bodied robots (Cowan and Walker, 2008).

In order to reproduce the undulatory body motion of fishes, smart materials appear to be extremely suited. In fact, over the last years, there has been an increasing activity in this field. Research in the field of smart materials for underwater locomotion is focused into mechatronics design and actuators control. As far as mechatronic design, much work is devoted to building hydrofoils using, e.g. piezo-electric fiber composite (Ming et al., 2009), embedding SMA wires into an elastic material such as silicone (Wang et al., 2008) or using SMAs as linear actuators (Rediniotis et al., 2002). Another big challenge is the control of such materials. Due to the novelty of smart materials

[1]Robotuna, a robot fish developed at MIT in 1994, had 2,843 parts controlled by six motors (font: MIT News, http://web.mit.edu/newsoffice/2009/robo-fish-0824.html)

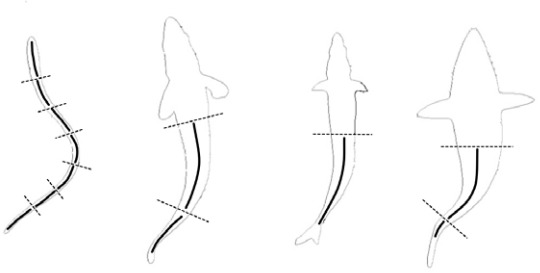

Figure 1: Different kinds of undulatory swimming: from left to right: anguilliform, subcarangiform, carangiform, thunniform. (Figure adapted from (Sfakiotakis et al., 1999).)

technology, the literature and the know-how regarding their use is still weak. In the case of SMAs, excellent results have been achieved by (Teh, 2008).

In this paper, we present our work on a swimming robot. In Section 2 we present a new mechatronic design which involves a continuous deformable structure, actuated by a discrete number of actuators made with SMA wires. In Section 3 we describe the low-level control electronics we have designed for the control of the actuators. Section 4 presents the results of the control electronics on the actuators. Finally, Section 5 concludes the paper with closing remarks on current and future work.

2 MECHATRONICS DESIGN

Fishes can swim bending their body in such a way to produce a backward-propagating propulsive wave. Such bending come in different ways (see Figure 1). Anguilliform swimmers show a snake-like motion: their body can be divided into numerous segments from head to tail and can reproduce at least one complete wavelength along the body. Conversely, subcarangifor, carangiform and thunniform swimmers only bends the second half of the body (roughly) and the number of segments is reduced to one or two (Sfakiotakis et al., 1999).

For our model, we have chosen to imitate the subcarangiform swimming style because of the reduced number of segments w.r.t. anguilliform fishes, which simplifies the study and the implementation, while having enough degrees of freedom that allow complex motion patterns to be reproduced. Our fish model can also bend the front part of its body, which makes a total of three bendable segments (cf. Fig. 2).

The fish is formed by a continuous structure made of polycarbonate of 1 mm thickness, which represents the fish backbone and spines. This material has been chosen for its temperature resistance, impact resistance and flexibility. Additional supporting structure is employed to support the silicon-based skin and gives the three-dimensional shape to the robot. The overall length of the fish is 30 cm (not including the caudal fin).

Along the spine, six SMA actuators are used to bend the body. Their length is $1/3$ body length (i.e. $8.5cm$, not counting the caudal fin and the head) and are positioned in pairs, in such a way to produce an antagonistic movement. Figure 3 shows a prototype of the structure and the location of the SMA wires. Thanks to this arrangement, the body segments can bend up to 30 degrees, regardless the fact that SMA wires only contracts a maximum of 4% of their length (cf. Fig. 4 and 8).The diameter size of the wires has been chosen as a trade-off between current consumption, pull force and contraction time. We have adopted a SMA with a diameter size of $150\mu m$ that has a pull force of 230 grams, a consumption of 250 mA at room temperature, and a nominal contraction time of 1 second. Such contraction time allows an undulation frequency of 1 Hz, which is enough for producing motion in water. Table 1 summarizes the characteristics of the SMA used [2].

Table 1: Summary of the characteristics of the SMA used.

Flexinol (nickel-titanium) SMA wire	
Diameter (μm)	150
Linear Resistance (Ωm)	50
Temperature (C)	90
Maximum Pull Force (grams)	230
Approx. Current at Room Temperature (mA):	250
Contraction Time (seconds)	1
Off Time at 90° C (seconds)	0.9

2.1 Shape Memory Alloys

SMAs are materials capable of changing their crystallographic structure (from *austensite* and *marteniste* phases), due to changes in temperature. These changes are reversible. When an SMA wire is subjected to an electrical current, Joule resistive heating causes the SMA actuator to contract. We have chosen SMAs because they have the advantage that they work at low currents and voltages, are extremely cheap and are easily available commercially. Nitinol, one of the most commercially available SMAs, is an

[2]The wires' speed and strain contraction depends on how fast and by how much the wire temperature is increased. In our tests, we have verified that SMAs wires can be fed with a current of up to $500mA$ without compromising their behavior.

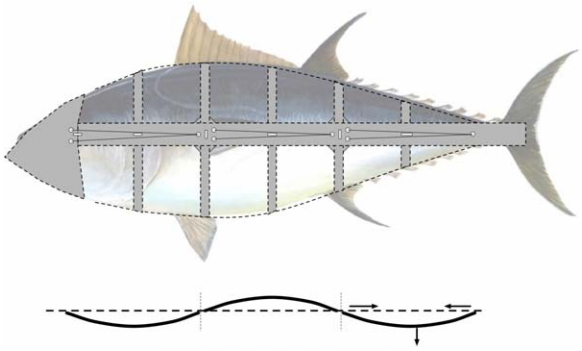

Figure 2: Lateral and upper view of the deformable structure.

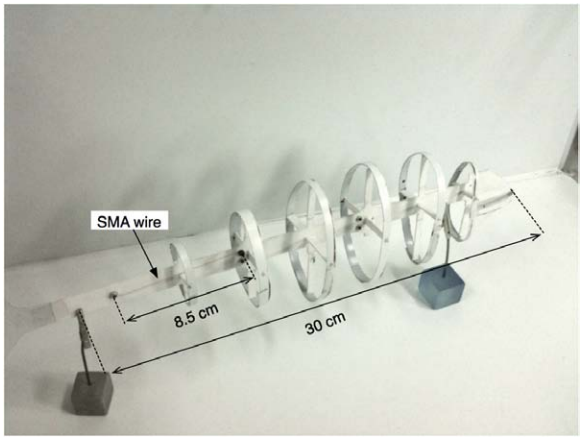

Figure 3: Prototype fish skeleton structure.

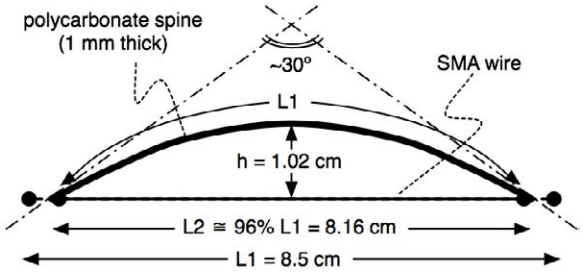

Figure 4: Principle of the bendable structure. The SMA wire is parallel to the spine segment. As it contracts, it causes the polycarbonate strip to bend.

alloy of nickel and titanium (NiTi). It is characterized by a high recovery stress ($> 500MPa$), low operational voltage ($4-5\ V$), a reasonable operational strain ($\approx 4\%$) and a long life (up to 10^6 cycles).

Piezoelectric (PZT) actuators are well known for their high efficiency and large force to mass ratio, but they have two main problems, the small strain and the high operating voltage (up to $1500V$). Electroactive polymers (EAP) also need very high voltage ($> 100\ MV/m$). Ionic polymermetal composite materials, one of the most sophisticated EAPs, has high efficiency and operational frequency, but is restricted by the problems of small stress, wetness maintaining and posture keeping under a DC voltage.

The behavior of SMAs is more complex than many common materials: the stress-strain relationship is non-linear, hysteretic, exhibits large reversible strains, and it is temperature dependent. For this reason, a low-level control electronics has to be designed in order to have a position control precise enough for the application at hand. A characteristics of SMAs is that they can also be used as sensors. In fact, once heated applying a given current, one can measure their resistance and calculate the actual percentage of shrinking. This measurement can be used as feedback for achieving precise position control.

3 SMA CONTROL

The SMA control electronics is conceived to be as simple as possible because of two main reasons. First, because we have to guarantee a quick answer and a minimum position error for the six actuators, and second because we do not want dedicate on-board CPU time to low-level control.

The control accuracy of smart actuators, such as SMAs or piezoceramic actuators is limited due to their inherent hysteresis nonlinearities (see Figure 5) with a local memory, resulting from the influence of a previous input on subsequent behavior. In addition, the existence of minor loops in the major loop because of a local memory also makes the mathematical modeling and design of a controller difficult for SMA actuators. Therefore, to enhance the controllability of a smart actuator, the Preisach hysteresis model (Visintin, 1995) has emerged as an appropriate behavioral model. Nevertheless, the modeling is difficult and the model equation is very complex. So even though this model is commonly used (Choi et al., 2004), the use of a heat transfer model and sensor hardware has been introduced.

However, SMAs provide the possibility to create controller systems without sensor hardware. The detection of inner electrical resistance allows to regulate the actuator movement (Ikuta et al., 1988). The method consists in measuring the electrical resistance of an SMA element (Teh, 2008), calculating a maximum safe heating current as a function of measured resistance, and ensuring that the actual heating current does not exceed this maximum value. In fact, resistance is being used as a form of temperature measurement, and the maximum safe heating current is

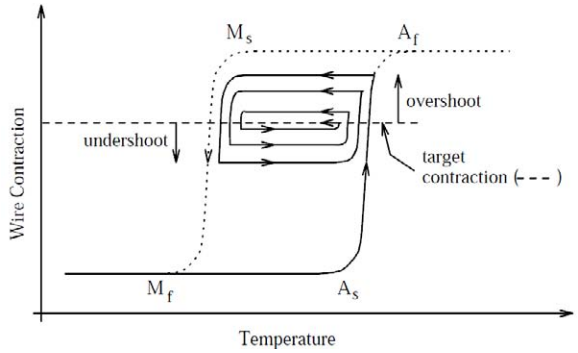

Figure 5: Histeresis of the SMA. (A_s, the austenite start temperature; A_f, the austenite finish temperature; M_s, the martensite start temperature; and M_f, the martensite finish temperature.)

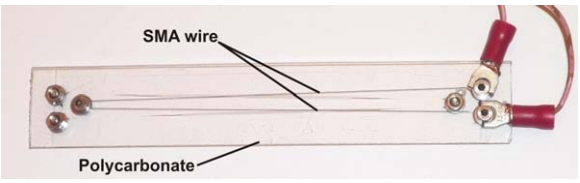

Figure 6: The test mock-up

designed to prevent overheating. Moreover, the hysteresis on the resistance curve is smaller than the hysteresis on the temperature curve, as shown in (Teh, 2003), which makes the linear approximation more accurate.

The maximum contraction of the wire can be measured as

$$\Delta L_{A_f} = \frac{L_{SMA_{Mf}} L_R - R_{SMA_{Af}}}{L_R}, \qquad (1)$$

where , $L_{SMA_{Mf}}(cm)$ is the SMA length in martensite finish temperature (relaxed SMA), $L_R(\Omega/m)$ is the linear resistance and $R_{SMA_{Af}}(\Omega)$ is the resistance at austenite finish temperature (i.e. at maximum contraction).

3.1 Design of PID by Ziegler-Nichols tuning rule for an SMA wire

In order to tune the control system, we set up a mock-up of a segment of the fish spine, corresponding to a $10 \times 2cm$ stripe of $1mm$ thick polycarbonate, with a $17cm$ long SMA wire in a V-shaped configuration, in order to double the pull force (see Figure 6). Figure 7 shows the answer to a $260mv$ step input, that corresponds to $300mA$ of SMA arousal. We used this value for tuning the PID controller because it allows a stable SMA response in open loop.

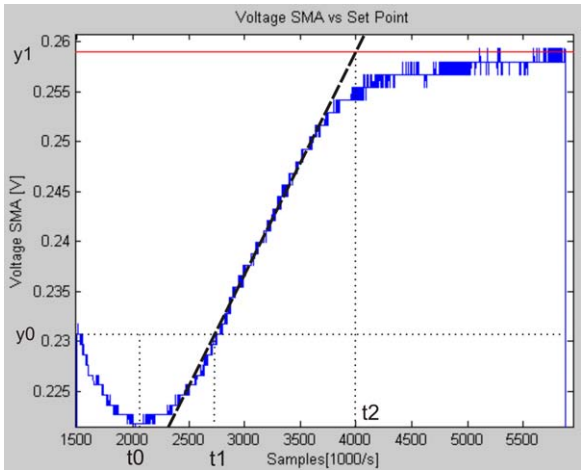

Figure 7: Voltage SMA vs. a given set point. $y_1 = 0.258, y_0 = 0.232, t_1 = 2.725 t_0 = 2.2 t_2 = 4 u_1 = 1 u_0 = 0$, experimentally determined.

One of the most common controllers that is used in the heat control is the PID (proportional-integral-derivative) controller, and responds to the equation

$$u(t) = K_p e(t) + \frac{K_p}{T_i} \int_0^t e(t)dt + K_p T_d \frac{de(t)}{dt}, \qquad (2)$$

where $e(t)$ is the signal error and $u(t)$ is the control input of the process. K_p is the proportional gain, T_i is the integral time constant and T_d is the derivative time constant. In the s domain, the PID controller can be written as

$$U(s) = K_p \left[1 + \frac{1}{T_i s} + T_d s \right] E(s). \qquad (3)$$

Following Ziegler-Nichols, we have tuned the values to the three parameters (K_p, T_i, T_d) of the PID controller based on the analysis of the open and close loop of the system to be controlled. At open loop a lot of systems can be defined according to the following transference function:

$$G(s) = \frac{K_0 e^{-s\tau_0}}{1 - s\gamma_0}, \qquad (4)$$

where the coefficients K_0, τ_0 and γ_0 are obtained of the response of the open loop system to a step input. We start of the stabilized system in $y(t) = y_0$ to $u(t) = u_0$; a step input is applied from u_0 to u_1. The exit answer is registered until it stabilizes at the new operation point (see Fig. 7).

From the experimental data corresponding to Figure 7, we can compute the following parameters:

$$\tau_0 = t_1 - t_0, \gamma_0 = t_2 - t_1, K_0 = (y_1 - y_0)/(u_1 - u_0).$$

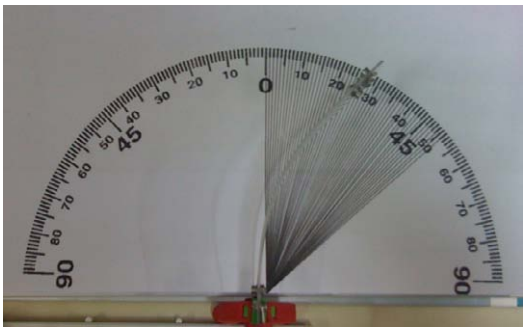

Figure 8: Maximum angle achieved, at a 350mA current.

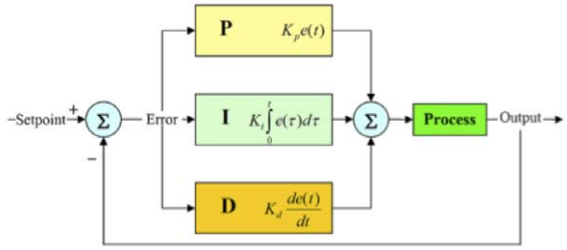

Figure 9: Block diagram of the PID controller used.

According to Ziegler-Nichols, the relations between these coefficients and the controller parameters are:

$$K_p = (1.2\gamma_0)/(K_0\tau_0), \quad T_i = 2T_0, \quad T_d = 0.5.$$

Then, according to the Z transform the discrete PID controller is:

$$U(z) = E(z)K_p\left[1 + \frac{T}{T_i(1-z^{-1})} + T_d\frac{1-z^{-1}}{T}\right]. \quad (5)$$

Also:

$$\frac{U(z)}{E(z)} = a + \frac{b}{1-z^{-1}} + c(1-z^{-1}). \quad (6)$$

Where:

$$a = Kp, \quad b = \frac{K_pT}{T_i}, \quad c = \frac{K_pT_d}{T}.$$

The parameters obtained were: $\tau_0 = 0.525, \gamma_0 = 1.276, K_0 = 0.03, K_p = 97.22, T_i = 1.05, T_d = 0.2625$. The discrete controller parameters are calculated based at the time $T = 0.1 < \tau_0/4$. Finally, $a = 97.22, b = 1.05, c = 255.202$.

The PID controller structure used is shown in Figure 9.

3.2 SMA control electronics

The control electronics has two stages. The first one is the conversion of the PWM signal delivered by the micro-controller to DC tension. The second is a Voltage Controlled Current Source that receives the DC tension and transforms it in a constant current that feeds the SMA. The second stage has been designed to have a low power consumption (7mA to 20mA when all the circuits are connected). The current that passes trough the SMA when it is resting is less than 3mA, which lets it cool quickly. Figure 10 shows the control block diagram and the electronics. The 6 fibers share the micro-controller and each one has an independent electronic circuit feed by the same power supply.

The voltage-controlled current source VCCS is used to generate a constant current in the SMA wire and to heat it constantly, the current varies according to the control DC tension that is related to the PWM duty cycle. The PWM duty cycle goes from 5% to 95% with a 1kHz frequency in order to avoid an excessive current on the SMA.

A problem associated to these kinds of designs is the integral windup, which can provoke long overshoot periods, encouraged by the excessive values that reaches the control sign due to the accumulation in the integrator.

In order to avoid this problem and accelerate the heating, (Teh, 2008) proposed to feed the SMA with a high pulse of current. However, while in (Teh, 2008) such pulse is maintained throughout the SMA excitation time, our control systems sends a high pulse of current only for a small period of time, precisely 500mA for 150mS. Then, it feeds the SMA with a normal ramp from 10% of the target current to 100% of the target current. Moreover, to reduce the over and undershoot, the voltage was limited between a minimum and maximum value of 10mV and 60mV, respectively, making the integrator act only when these limits are overcome (cf. Fig. 11). Such values have been determined experimentally.

The hardware used (18F458 PIC) has a 10-bits A/D converter. Since in our system the maximum voltage measured at the SMA is $V_{SMA} = 0.55V$, with a 10 bits encoding we will have a resolution of

$$\frac{V_{SMA}}{2^{10}-1} = 0.537mV.$$

Thus, taking into consideration the maximum current through the wire (500mA) we can measure the SMA resistances variations of 1.074$m\Omega$. Since the maximum variation in the SMA length is of 0.34cm and the maximum variation of the resistance is of 1.6Ω, the system theoretical error on the SMA length is of 0.067%. i.e. 0.0023mm.

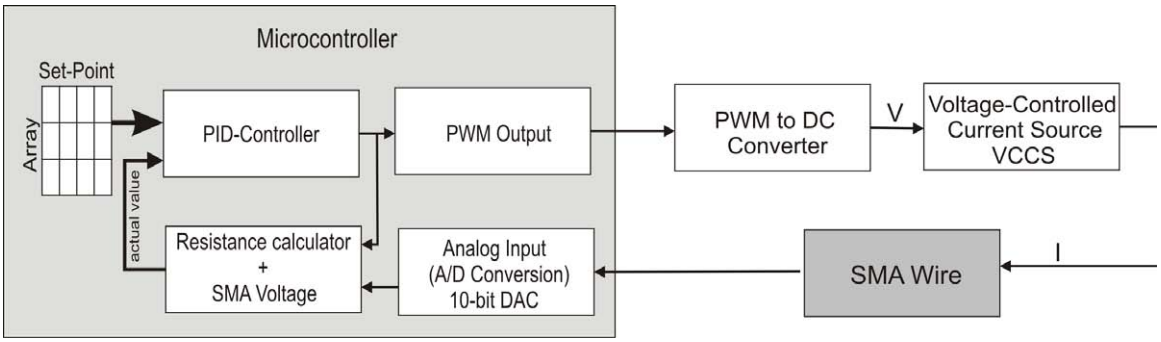

Figure 10: Control loop of a single SMA actuator.

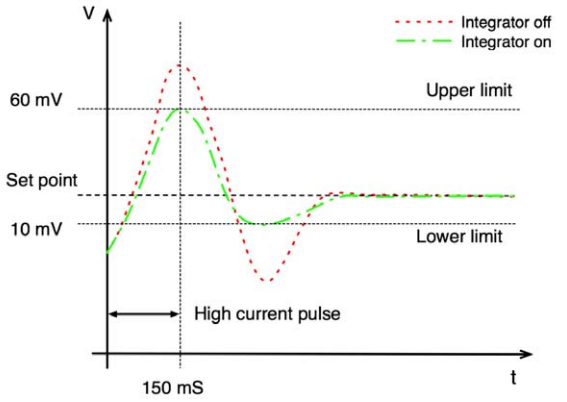

Figure 11: Typical behavior of the control signal.

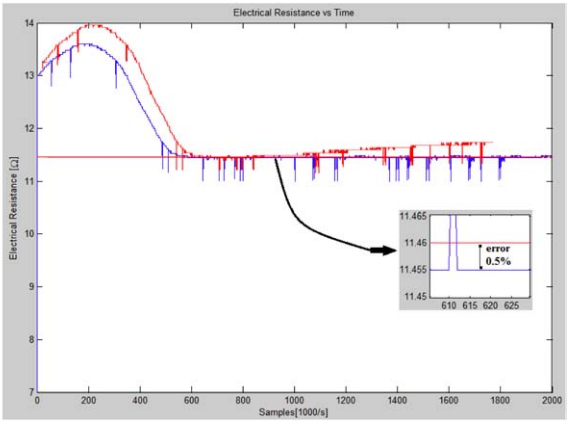

Figure 12: Transient performance for a 11.46Ω set point.

4 EXPERIMENTAL RESULTS

Using the mock-up mentioned above, we have tested the control system by applying different target resistances (i.e. desired lengths). Given the small displacements, it is very difficult to measure with sufficient precision the final length of the wire. Therefore, in order to assess the actual precision of the system we have measured the final resistance of the SMA wire.

Figure 12 shows the transient performance for a 11.46Ω set point corresponding to a 3.08*mm* SMA contraction. With a 450*mA* current we get a settling time of 0.43*s*. The overshoot that can be noticed in the plot is produced by the initial pulse. Note how, thanks to the action of the integrator, the overshoot is reduced (blue plot) w.r.t the behavior of the SMA without it (red plot). In the zoomed part the actual precision error of 0.5% can be noticed. Figure 12 shows the comparison of the transient period for two different currents, which is very similar.

Table 2 summarizes the results for various set points (target resistance). As it can be noticed, the precision obtained is very good, although higher than the one theoretically achievable. On the practical point of view the precision obtained is satisfactory for the purposes of our mechatronic system, since it corresponds to a sub-millimeter position error. Such error translates into a bending error (height *h* of Fig. 4) which is negligible for the mechanics of swimming.

Table 2: Summary of the performances of the control.

Target resistance (Ω)	Settling time (s)	Resistance error (%)	Length error (mm)
12.5	0.274	3	0.102
12.4	0.302	2	0.068
12.2	0.316	1	0.034
12 .0	0.331	5	0.170
11.8	0.353	1	0.034
11.6	0.374	5	0.170
11.46	0.43	0.5	0.017

5 CONCLUSIONS

We have presented our current work on bio-inspired locomotion for underwater robots. The objective of this work is to investigate the use of active materials such as SMAs as alternative actuation

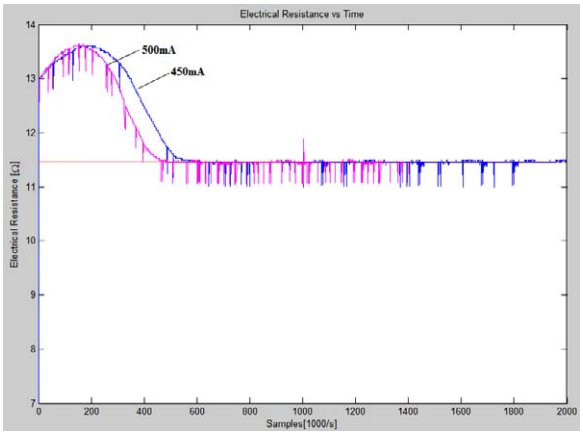

Figure 13: Comparison of the transient period at 450mA and 500mA.

system for such kind of motion. This paper is focussed on the SMA control and control electronics. The long-term aim of our work is to move towards soft-bodied robots. For this reason we designed a continuous deformable structure. The main advantage of this mechatronics design is its simplicity, extremely light weight and practically null volume, at advantage of the available payload. Moreover, the actuators are absolutely silent and do not produce any vibration, a feature which can be exploited, e.g. in the observation of sea wild life since the robot would not disturb in any way (besides its presence).

Smart materials pose new challenges as far as fine control is concerned. We have achieved a position control for the SMAs that is accurate enough for the application at hand, since produces an error that is negligible as far as undulatory motion of the fish parts. Nevertheless, for applications where more precision is needed (e.g. manipulation) more accurate controllers are needed.

Current work is aimed at the miniaturization of the electronics using SMD technology. Each of the six controllers will have the dimension of a SIMM card and will be hosted onboard. At the same time, we are experimenting the skin of the fish using silicone and latex. Once the electronics will be embedded in the structure, and the fish protected by the skin, the next step will be testing in water to compare the results of the simulations with the real behavior.

In conclusion, we believe that smart actuators and flexible continuous structures can be a promising field for making alternative robots, that are simpler and lighter, and that can have interesting application domains.

REFERENCES

Anderson, J. M. and Chhabra, N. K. (2002). Maneuvering and stability performance of a robotic tuna. *Integrative and Comparative Biolog*, 42(1):118–126.

Choi, B.-J., Lee, Y.-J., and Choi, B.-Y. (2004). Fast preisach modeling method for shape memory alloy actuators using major hysteresis loops. *Smart Mater. Struct.*, 23:1069–1080.

Cowan, L. and Walker, I. (2008). Soft continuum robots: The interaction of discrete and continuous elements. In *Artificial Life XI*, pages 126–133.

de Santos, J. G., Cobano, J. A., Garcia, E., Estremera, J. ., and Armada, M. (2007). A six-legged robot-based system for humanitarian demining missions. *Integrative and Comparative Biolog*, 17:417–430.

Hu, H. (2006). Biologically inspired design of autonomous robotic fish at essex. In *IEEE SMC UK-RI Chapter Conference, on Advances in Cybernetic Systems*, pages 3–8.

Ikuta, K., Tsukamoto, M., and Hirose, S. (1988). Shape memory alloy servo actuator system with electric resistance feedback and application for active endoscope. In *IEEE International Conference on Robotics and Automation*, pages 423–430.

Ming, A., Park, S., Nagata, Y., and Shimojo, M. (2009). Development of underwater robots using piezoelectric fiber composite. In *IEEE International Conference on Robotics and Automation*.

Morgansen, K., Triplett, B., and Klein, D. (2007). Geometric methods for modeling and control of free-swimming fin-actuated underwater vehicles. *IEEE Transactions on Robotics*, 23(6):1184–1199.

Rediniotis, O. K., Wilson, L. N., Lagoudas, D. C., and Khan, M. M. (2002). Development of a shape-memory-alloy actuated biomimetic hydrofoil. *Journal of Intelligent Material Systems and Structures*, 13(1):35–49.

Sfakiotakis, M., Lane, D. M., and Davies, J. B. C. (1999). Review of fish swimming modes for aquatic locomotion. *IEEE journal of oceanic engineering*, 24(2):235–252.

Teh, Y. H. (2003). *A Control System for Achieving Rapid Controlled Motions From Shape Memory Alloy (SMA) Actuator Wires*. PhD thesis, Dept. Engineering, The Australian National University.

Teh, Y. H. (2008). An architecture for fast and accurate control of shape memory alloy actuators. *International Journal of Robotics Research*, 27(5):595–611.

Valdivia y Alvarado, P. and Youcef-Toumi, K. (2006). Design of machines with compliant bodies for biomimetic locomotion in liquid environments. *ASME Journal of Dynamic Systems, Measurement, and Control*, 128:3–13.

Visintin, A. (1995). *Differential Models of Hysteresis*. Applied Mathematical Sciences. Springer, Berlin.

Wang, Z., Hang, G., Wang, Y., Li, J., and Du, W. (2008). Embedded sma wire actuated biomimetic fin: a module for biomimetic underwater propulsion. *Smart Materials and Structures*, 17(2):25–39.